

Confining Strings in Supersymmetric Theories with Higgs Branches

M. Shifman,^a Gianni Tallarita,^b and Alexei Yung^{a,c}

^a*William I. Fine Theoretical Physics Institute, University of Minnesota,
Minneapolis, MN 55455, USA*

^b*Centro de Estudios Científicos (CECs), Casilla 1469, Valdivia, Chile*

^c*Petersburg Nuclear Physics Institute, Gatchina, St. Petersburg 188300,
Russia*

Abstract

We study flux tubes (strings) on the Higgs branches in supersymmetric gauge theories. In generic vacua on the Higgs branches strings were shown to develop long-range “tails” associated with massless fields, a characteristic feature of the Higgs branch (the only exception is the vacuum at the base of the Higgs branch). A natural infrared regularization for the above tails is provided by a finite string length L .

We perform a numerical study of these strings in generic vacua. We focus on the simplest example of strings in $\mathcal{N} = 1$ supersymmetric QED with the Fayet-Iliopoulos term. In particular, we examine the accuracy of a logarithmic approximation (proposed earlier by Evlampiev and Yung) for the tension of such string solutions. In the Evlampiev-Yung formula the dependence of tension on the string length is logarithmic and the dependence on the geodesic length from the base of the Higgs branch is quadratic. We observe a remarkable agreement of our numerical results for the string tension with the Evlampiev-Yung analytic expression.

1 Introduction

Supersymmetric gauge theories provide an excellent theoretical laboratory for understanding strongly coupled non-Abelian dynamics. In particular, the dual Meissner effect as a mechanism of confinement suggested in the mid-1970s [1] was first analytically observed in 1994 in the framework of $\mathcal{N} = 2$ supersymmetric theories [2, 3]. The main feature of this mechanism is formation of the Abrikosov-Nielsen-Olesen (ANO) [4] flux tubes (confining strings). If in a given vacuum quarks condense then the conventional magnetic ANO strings are formed. They confine monopoles. If, instead, monopoles condense, the electric ANO strings are formed. They confine quarks [2, 3] (see also [5, 6] for reviews of scenarios with confined monopoles).

Quite often supersymmetric gauge theories have Higgs branches. These are flat directions of the scalar potential on which charged scalar fields can develop vacuum expectation values (VEVs) breaking the gauge symmetry. In many instances this breaking provides topological reasons behind formation of the ANO strings. The dynamical side of the problem of the confining string formation in the theories with Higgs branches was addressed in [7, 8, 9]. *A priori* it is not clear at all whether or not stable string solutions exist in this class of theories. The point is that the theories with a Higgs branch represent a limiting case of type I superconductor, with vanishing Higgs mass. In particular, it was shown in [7] that infinitely long strings cannot be formed in this case due to infrared divergences.

Later this problem was studied [8] in a more realistic confinement setup, namely, the string in question was assumed to have a large but finite length L . Finite length provides an infrared regularization implying [8] that finite-size ANO strings still exist on the Higgs branches. They become logarithmically “thick” due to the presence of massless fields and give a confining potential for two heavy trial charges of the form

$$V(L) \sim \frac{L}{\log L}. \quad (1)$$

Note that $V(L)$, instead of being linear in separation L is modified by $\log(L\Lambda)$ in the denominator.

The potential between heavy trial charges provides us with an order parameter marking distinct phases with different dynamical behaviors. Thus, we see that theories with the Higgs branches develop a novel confining phase with logarithmically nonlinear potential (1).

Formation of strings in more generic theories with non-flat Higgs branches curved by the presence of the Fayet-Iliopoulos (FI) term was considered later in [9]. In this case string profile functions can be approximated by an almost BPS core built from massive fields and a long-range “tail” built from massless fields. In this approximation the confining potential for the simplest case of the $U(1)$ $\mathcal{N} = 1$ supersymmetric gauge theory with one flavor of charged matter was shown to be

$$V(L) \sim L \left(1 + \frac{l^2}{\log L} \right), \quad (2)$$

where l is the length of the geodesic line on the Higgs branch between the given vacuum and the base point of the Higgs branch.

In this paper our task is to confirm the onset of the regime (2) for sufficiently large L . This will allow us to better understand the limits of applicability of the analytic consideration in [9]. To this end we numerically study the string solution in $\mathcal{N} = 1$ supersymmetric QED with the FI term. We find the string profile functions and calculate the string tension. In agreement with the analytic formula (2) we observe that our numeric solution reproduces (with good accuracy) both features: the logarithmic dependence of the “tail” tension on L and the quadratic dependence on l .

The paper is organized as follows. In Sec. 2 we briefly review a basic construction of length- L flux tubes on curved Higgs branches in $\mathcal{N} = 1$ SQED. Then we summarize main results concerning the analytic approximation [9] for their tension in terms of the distance from the base of the Higgs branch and L . In Sec. 3 we obtain the full numerical result for the profile functions of the string solution following the general guidelines of [8]. We then put the analytical tension formula (2) to test. Our numeric data establishes the onset of the analytic approximation (2). In Sec. 4 we present some conclusions.

2 Flux tubes on curved Higgs branches

2.1 $\mathcal{N} = 1$ supersymmetric QED

We begin by reviewing the construction of flux tubes on curved Higgs branches in the Abelian gauge theories [8, 9]. The starting point is $\mathcal{N} = 1$ SQED with the action

$$S_{\text{QED}} = \int d^4x \left(\frac{1}{4g^2} F_{\mu\nu}^2 + |D_\mu q|^2 + |D_\mu \tilde{q}|^2 + V(q, \tilde{q}) \right) \quad (3)$$

where the covariant derivative is defined as

$$D_\mu = \partial_\mu - \frac{i}{2} A_\mu \quad (4)$$

and the complex scalar fields q and \tilde{q} have opposite charges under the $U(1)$ gauge symmetry. We assume the charges for the scalar fields n_e to be $|n_e| = 1/2$. The scalar potential is

$$V(q, \tilde{q}) = \frac{g^2}{8} (|q|^2 - |\tilde{q}|^2 - \xi)^2. \quad (5)$$

It is obtained from the Fayet-Iliopoulos (FI) coupling for the $U(1)$ vector superfield with FI parameter ξ after its auxiliary field D is integrated out.

This model has a rich vacuum structure dictated by the vacuum condition

$$|\langle q \rangle|^2 - |\langle \tilde{q} \rangle|^2 - \xi = 0, \quad (6)$$

which describes a Higgs branch of dimension two: two complex scalars subject to one constraint after reduction of a gauge phase. As is clear from the condition (6) in the vacuum the scalar fields develop vacuum expectation values thus completely breaking the $U(1)$ gauge symmetry. Correspondingly the photon acquires the mass

$$m_\gamma = \frac{1}{2} g^2 v^2, \quad (7)$$

where

$$v^2 = |\langle q \rangle|^2 + |\langle \tilde{q} \rangle|^2. \quad (8)$$

The scalar mass matrix has three zero eigenvalues corresponding to one “eaten” combination and two massless scalar components of chiral multiplets living on the Higgs branch. In addition, the mass matrix has one non-zero eigenvalue corresponding to a massive scalar field which is the superpartner of the massive vector supermultiplet, with mass equal to the mass of the photon $m_H = m_\gamma$.

Consider now the low-energy effective action for the theory (3), see [9]. To integrate out all massive fields in (3), namely, the photon and the heavy scalar, we use the following parametrization of the Higgs branch:

$$q = \sqrt{\xi} e^{i(\alpha+\beta)} \cosh(\rho), \quad (9)$$

$$\tilde{q} = \sqrt{\xi} e^{i(\alpha-\beta)} \sinh(\rho), \quad (10)$$

where $\rho(x)$, $\alpha(x)$ and $\beta(x)$ are three real fields parametrizing q and \tilde{q} subject to condition (6). Once the gauge field is massive at low energies we can neglect its kinetic term and eliminate A_μ using the algebraic equation

$$A_\mu = -i \frac{\bar{q} \partial_\mu q - \partial_\mu \bar{q} q + \tilde{q} \partial_\mu \bar{\tilde{q}} - \partial_\mu \tilde{q} \bar{\tilde{q}}}{|q|^2 + |\tilde{q}|^2} = 2 \left(\partial_\mu \alpha + \frac{\partial_\mu \beta}{\cosh 2\rho} \right). \quad (11)$$

Substituting this into the action (3) we arrive at

$$S_{\text{eff}} = \xi \int d^4x \cosh 2\rho \left\{ (\partial_\mu \rho)^2 + (\partial_\mu \beta)^2 \tanh^2 2\rho \right\}. \quad (12)$$

This is the low energy-action in SQED, see (3), containing only massless fields on the Higgs branch. The gauge phase $\alpha(x)$ is canceled out as expected.

In the simplest case, at the base of the Higgs branch, the vacuum is

$$\langle \tilde{q} \rangle = 0, \quad \langle q \rangle = \sqrt{\xi}. \quad (13)$$

Far away from the base we can parametrize vacua on the Higgs branch as follows:

$$\begin{aligned} \langle q \rangle &= \sqrt{\xi} e^{i\beta_0} \cosh(\rho_0), \\ \langle \tilde{q} \rangle &= \sqrt{\xi} e^{-i\beta_0} \sinh(\rho_0). \end{aligned} \quad (14)$$

Here $\rho_0 = \rho(\infty)$ is a real dimensionless parameter describing how far the given vacuum lies from the base of the Higgs branch at $\rho_0 = 0$, while β_0 is the residual phase which cannot be gauged away. Each vacuum on the Higgs branch is characterized by two parameters ρ_0 and β_0 .

2.2 String solutions

Consider first the vacuum (13) located on the base of the Higgs branch. This vacuum admits the standard Abrikosov-Nielsen-Olesen vortices of infinite length [4] in which the phase of the scalar field q winds while its absolute value rapidly tends to its vacuum expectation value at spatial infinity. These strings are BPS saturated, with the tension

$$T_{\text{BPS}} = 2\pi n \xi. \quad (15)$$

Here n the winding number of the solution. Below we consider elementary strings with $n = 1$.

As was mentioned, in this paper we are interested in the flux tube solutions at a generic point on the Higgs branch. Such solutions can be found through the procedure of dividing the radial separation from the string center into two distinct spatial domains suggested in [9].

First, one can safely assume that the photon field and the massive scalar field will form a BPS core of a finite radius determined by their common mass, namely,

$$R_c \sim 1/g\sqrt{\xi}.$$

This implies that for $r \leq R_c$ we can look for the solutions in which $\tilde{q} \approx 0$. This domain is described by the standard BPS ANO string for which $T = T_{\text{BPS}}$.

Second, outside the above core, at $r \geq R_c$, the photon field vanishes. However, the massless fields are excited, and their dynamics is determined by the low-energy action (12). This leads to a long-range logarithmic tail, contributing both, to the profile functions and the string tension [9].

The above long-range logarithmic tails require an infrared (IR) regularization. This statement is equivalent to the well-known result that the infinite-length strings are not allowed on Higgs branches [7]. We will regularize our solutions by considering strings of a finite length L .

The finite length IR regularization is physically motivated because it corresponds to considering the string in the confinement setup. Namely, we assume that finite length string is stretched between infinitely heavy trial monopole and antimonopole at separation L . As we already mentioned the problem with infinite string arises because at large r outside the string core scalar fields satisfy free equations of motion and therefore, have logarithmic behavior in two dimensions. Now for the case of the finite length string scalar fields also have logarithmic tails for $R_c \ll r \ll L$. However, as r becomes of order of the string length L the problem becomes three-dimensional rather than two-dimensional, see [8] for details. In three dimensions solution of the free equation of motion for the scalar field behaves as $1/|x_n|$ (rather than $\log r$), where x_n , $n = 1, 2, 3$ are the coordinates in the three-dimensional space. These solutions can reach their boundary values at infinity dictated by (14). Thus, $1/L$ plays the role of the IR regularization for the logarithmic behavior of scalar fields at large r . In other words the finite length L along the string axis translates into the IR regularization in the plane orthogonal to the string axis.

The total tension of the finite- L solutions will be given by

$$T = T_{\text{BPS}} + T_{\text{tail}}, \tag{16}$$

where T_{tail} denotes the contribution to the tension from the long-range tail. It is given by

$$T_{\text{tail}} = \xi \int d^2x \cosh 2\rho \left[(\partial_i \rho)^2 + (\partial_i \beta)^2 \tanh^2 2\rho \right], \quad (17)$$

where we assume that the string is a static solution aligned along the x^3 axis, so the string profile functions in (17) depend only on coordinates x^i with $i = 1, 2$, if $r \ll L$.

Although the tail profile function were not found in [9] it was shown that the tail tension is determined by the universal formula depending on the length l of the geodesic line from the given vacuum to the base of the Higgs branch. In our model this length reduces to

$$l = \int_0^{\rho_0} \sqrt{\cosh(2\rho)} d\rho, \quad (18)$$

where the upper limit is the position of the vacuum on the Higgs branch, see (14). The final result for strings of length L (in the limit $L \gg R_c$) is

$$T_{\text{tail}} \approx \frac{2\pi\xi}{\log(g\sqrt{\xi}L)} l^2, \quad (19)$$

see [9] for a detailed derivation. Hence, the expression for the total tension (16) is

$$\frac{T}{2\pi\xi} \approx 1 + \frac{1}{\log(g\sqrt{\xi}L)} l^2. \quad (20)$$

Formation of such strings leads to confinement of monopoles with the confining potential (2). It is not strictly linear in L .

Another IR regularization more suitable for numerical calculations is to lift the Higgs branch giving massless fields a small mass without breaking $\mathcal{N} = 1$ supersymmetry. One particular way to do this is considered in [9]. One can start from $\mathcal{N} = 2$ QED and deform it with the mass term μ for the neutral chiral multiplet. This term breaks $\mathcal{N} = 2$ supersymmetry down to $\mathcal{N} = 1$ and at large masses μ the deformed theory flows to $\mathcal{N} = 1$ QED. Integrating out the massive neutral multiplet one obtains the scalar potential

$$V(q, \tilde{q}) = \frac{g^2}{8} (|q|^2 - |\tilde{q}|^2 - \xi)^2 + \frac{1}{4\mu^2} (|q|^2 + |\tilde{q}|^2) \left| q\tilde{q} - \frac{\eta}{2} \right|^2, \quad (21)$$

where η is a new parameter which we take to be real, see [9, 10] for details. We will consider this potential as an IR regularization of the one in (5). The Higgs branch is now lifted and we have an isolated vacuum with the vacuum value ρ_0 given by

$$\sinh 2\rho_0 = \frac{\eta}{\xi} \quad (22)$$

The light scalar fields ρ and β in the low-energy action (12) are no longer massless. They acquire the mass

$$m_L = \frac{v^2}{2\mu}, \quad (23)$$

where v is the VEV given by (8). In terms of parameters of the potential (21) v can be expressed as

$$v^4 = \xi^2 + \eta^2. \quad (24)$$

The relation between the two IR regularizations introduced above is

$$m_L \sim \frac{1}{L}, \quad (25)$$

and the result (20) for the string tension reads

$$\frac{T}{2\pi\xi} \approx 1 + \frac{l^2}{\log(g\sqrt{\xi}/m_L)}. \quad (26)$$

We use the latter IR regularization for the numerical calculations below. This regularization allows us to consider infinitely long string and look for solutions for the string profile functions in (x^1, x^2) plane.

3 Numerical solutions

In this section we will construct full numerical solutions describing strings at a generic point on the Higgs branch and, with these solutions in hand, we can directly verify the validity of the Evlampiev-Yung analytic formula (26). Our numerical solver involves a second order central finite difference procedure with accuracy $\mathcal{O}(10^{-4})$. From here on we set

$$g = 1.$$

It is convenient to define dimensionless quantities as

$$\rho = \sqrt{\xi} r, \quad \tilde{\mu}^2 = \frac{\mu^2}{\xi}, \quad \tilde{\eta} = \frac{\eta}{\xi}. \quad (27)$$

Then the energy minimization equations, after using the *ansatz*

$$\begin{aligned} A_0 &= A_r = 0, & A_\theta &= 2(1 - f(\rho)), \\ q &= \sqrt{\xi} q(\rho) e^{i\theta}, \\ \tilde{q} &= \sqrt{\xi} \tilde{q}(\rho) e^{-i\theta}, \end{aligned} \quad (28)$$

reduce to

$$\begin{aligned} q'' + \frac{q'}{\rho} &= \frac{1}{\rho^2} q f^2 + \frac{1}{4} (q^2 - \tilde{q}^2 - 1) q \\ &+ \frac{1}{4\tilde{\mu}^2} \left(q\tilde{q} - \frac{\tilde{\eta}}{2} \right) \left[q \left(q\tilde{q} - \frac{\tilde{\eta}}{2} \right) + \tilde{q} (q^2 + \tilde{q}^2) \right], \\ \tilde{q}'' + \frac{\tilde{q}'}{\rho} &= \frac{1}{\rho^2} \tilde{q} f^2 - \frac{1}{4} (q^2 - \tilde{q}^2 - 1) \tilde{q} \\ &+ \frac{1}{4\tilde{\mu}^2} \left(q\tilde{q} - \frac{\tilde{\eta}}{2} \right) \left[\tilde{q} \left(q\tilde{q} - \frac{\tilde{\eta}}{2} \right) + q (q^2 + \tilde{q}^2) \right], \\ f'' &= \frac{1}{2} f (q^2 + \tilde{q}^2) + \frac{f'}{\rho}, \end{aligned} \quad (29)$$

where prime denotes differentiation with respect to ρ and θ is the polar angle in (x^1, x^2) plane.

For large regularization parameter $\tilde{\mu}$, far from the base of the Higgs branch, where $f = 0$, the solution is basically determined by the Higgs constraint

$$q^2 - \tilde{q}^2 - 1 = 0. \quad (30)$$

Then, as is easily seen from Eqs. (29), the fields q and \tilde{q} obey the free equations of motion,

$$(\rho q')' = 0, \quad (\rho \tilde{q}')' = 0, \quad (31)$$

with the standard logarithmic solutions. Correspondingly, the tension of the flux tube will be dominated by this large logarithmic tail. Numerically the

ρ_0	l
0.2	0.20
0.4	0.42
0.6	0.67
0.8	0.96
1.0	1.32

(a)

$m_L/\sqrt{\xi}$	$\log(\sqrt{\xi}/m_L)$	$\tilde{\mu}_{0.2}$	$\tilde{\mu}_{0.3}$
0.05	2.99	10.81	11.85
0.033	3.40	16.22	17.78
0.025	3.69	21.62	23.71
0.020	3.91	27.03	29.64
0.017	4.09	32.43	35.56

(b)

Figure 1: Numerical values of (a) l and (b) $\log(\sqrt{\xi}/m_L)$ for characteristic parameters used in the numerical solutions. We put $g = 1$. $\tilde{\mu}_{0.2}$ and $\tilde{\mu}_{0.3}$ show the values of $\tilde{\mu}$ at $\rho_0 = 0.2$ and 0.3 for the values of m_L used in the table.

strategy is the following: the IR regularization is implemented as a mass regularization on the scalar fields, as explained in section 2. Then, once we fix m_L (making sure that $m_L \ll m_\gamma$) we impose boundary conditions on the fields at a fixed radial distance $R \gg 1/m_L$. In this scheme, in which we fix R we must ensure that ρ_0 is sufficiently small so that the BPS core approximation holds. If ρ_0 becomes too large then the \tilde{q} field will develop in the core and spoil the theoretical approximation.

We are interested in solutions of (29) with the following boundary conditions:

$$\begin{aligned}
q(0) &= \tilde{q}(0) = 0, \\
q(R) &= \cosh(\rho_0), \quad \tilde{q}(R) = \sinh(\rho_0), \\
f(0) &= 1, \quad f(R) = 0.
\end{aligned} \tag{32}$$

Figure 1 includes reference tables for the numerical values of the parameters l and $\log(\sqrt{\xi}/m_L)$ for characteristic values of ρ_0 and m_L used below. Solutions for the field profiles are shown in Figures 2 and 3 for varying values of m_L and ρ_0 . We fix $\sqrt{\xi}R = 120$. Some important expected features can be seen in these plots: there is a BPS core formed by the photon field and the field q ; in this domain the field \tilde{q} almost vanishes; outside the BPS core the gauge field vanishes, and the massless scalar fields exhibit large logarithmic tails.

Figures 4 and 5 show the results of the numerical analysis of the tension formula (20). As seen from the plots, at larger values of the parameters we find that for some particular combinations the accuracy of our procedure is

not enough to find a solution. These points are excluded from the plots. The results involve the difference between the numerical result for the tension and its BPS part coming from the core,

$$\frac{\Delta T}{\xi} = \frac{T - T_{\text{BPS}}}{2\pi\xi} = \frac{1}{\log(g\sqrt{\xi}/m_L)} l^2. \quad (33)$$

In particular, Fig. 4 shows a plot of $\sqrt{\Delta T/\xi}$ in which we fix m_L and vary l . We observe a number of important features.

First, the numerical and theoretical results coincide (within numerical accuracy) at $\rho_0 = 0$. This is expected, of course, since at this point we are at the base of the Higgs branch and the tension coincides with the BPS result. As we move along the Higgs branch by increasing ρ_0 we see an increasing disagreement between the numerical solution and the analytic (approximate) theoretical prediction. Once again, this is expected as in this domain one picks up large l effects. Second, we observe that the numerical solution for $\sqrt{\Delta T/\xi}$ is a linear function of l , in perfect agreement with the theoretical expression. A slight deviation in the slope can be explained by the logarithmic accuracy in the denominator in the theoretical prediction, the $\log(\sqrt{\xi}/m_L)$ term in the denominator can be shifted by a constant non logarithmic term of the order of unity. In fact, this conjecture is supported by the subsequent plots.

Figure 5 shows similar plots in which we fix ρ_0 in order to verify the logarithmic dependence on m_L . Once again, by observing the linear dependence in the plot, we verify that the logarithm dependence up to small values of m_L . Given that the theoretical approximation is for large values of logarithm in (26) it is not surprising to find a better agreement as m_L decreases (and thus $1/\log(\sqrt{\xi}/m_L)$ decreases). Quantitatively we find that at the smallest value of m_L the agreement between the theoretical T_{theor} and numerical T_{number} results, respectively is

$$\frac{T_{\text{number}} - T_{\text{theor}}}{T_{\text{number}}} \times 100 \approx 10\%, \quad (34)$$

(this value holds for both values of ρ_0 investigated). The agreement is quite satisfactory given the magnitude of the parameters used at this point (see Fig. 1). Adding a non-logarithmic term in the denominator of the theoretical expression and fitting it we could have dramatically improved the agreement (by two orders of magnitude!).

Indeed, since Eq. (20) is an approximation with logarithmic accuracy we propose a simple modification of this formula which we can test numerically. Let us replace (20) by

$$\frac{T}{2\pi\xi} \approx 1 + \frac{1}{\log(\sqrt{\xi}/m_L) - c} l^2, \quad (35)$$

where c is a constant to be fitted numerically. We find that, for $\rho_0 = 0.2$ and $R = 120$

$$\frac{T_{\text{numer}} - T_{\text{theor}}}{T_{\text{numer}}^c} \times 100 \approx 0.4\%, \quad (36)$$

provided that

$$c \approx 0.55.$$

In other words, the value of the non-logarithmic constant in (35) turns out to be less than one, a complete success. For values of ρ_0 greater than those used in the plots we find that one cannot ignore the effects of the \tilde{q} field in the core.

4 Conclusions

In this paper we analyzed magnetic flux tubes (strings) on the Higgs branch in supersymmetric QED. In generic vacua on the Higgs branches these strings were previously shown to develop long-range tails due to massless fields existing on the Higgs branch. A natural infrared regularization for the above tails can be provided by a finite string length L . Numerically a small supersymmetry preserving mass regularization was used, the two being related by $m_L \sim 1/L$.

We performed a detailed numerical analysis of flux tube solutions at generic points on the Higgs branch in $\mathcal{N} = 1$ SQED. We found numerical solutions for the field profile functions defining such strings that (i) contain a BPS core and (ii) besides the core contain long logarithmic tails due to the massless scalar fields characteristic to the Higgs branch. Using these solutions we then analyzed the Evlampiev-Yung analytic formula (26) (presenting the small- m_L geodesic approximation for the tail contribution to the string tension) comparing it to numerical results. We found good agreement for the predicted functional dependence on m_L and l .

Acknowledgments

This work is supported in part by DOE grant de-sc0011842 and Fondecyt grant No. 3140122. G.T. would like to thank the William I. Fine Theoretical Physics Institute of the University of Minnesota for hospitality during completion of this work. The work of A.Y. was supported by William I. Fine Theoretical Physics Institute of the University of Minnesota, by Russian Foundation for Basic Research under Grant No. 13-02-00042a and by Russian State Grant for Scientific Schools RSGSS-657512010.2. The work of A.Y. was supported by Russian Scientific Foundation under Grant No. 14-22-00281. The Centro de Estudios Científicos (CECS) is funded by the Chilean Government through the Centers of Excellence Base Financing Program of Conicyt.

References

- [1] Y. Nambu, Phys. Rev. D **10**, 4262 (1974);
G. 't Hooft, *Gauge theories with unified weak, electromagnetic and strong interactions*, in Proc. of the E.P.S. Int. Conf. on High Energy Physics, Palermo, 23-28 June, 1975 ed. A. Zichichi (Editrice Compositori, Bologna, 1976); Nucl. Phys. B **190**, 455 (1981); S. Mandelstam, Phys. Rept. **23**, 245 (1976).
- [2] N. Seiberg and E. Witten, *Electric - magnetic duality, monopole condensation, and confinement in $\mathcal{N} = 2$ supersymmetric Yang-Mills theory*, Nucl. Phys. **B426**, 19 (1994), (E) **B430**, 485 (1994) [hep-th/9407087].
- [3] N. Seiberg and E. Witten, *Monopoles, duality and chiral symmetry breaking in $\mathcal{N} = 2$ supersymmetric QCD*, Nucl. Phys. **B431**, 484 (1994) [hep-th/9408099].
- [4] A. Abrikosov, Sov. Phys. JETP **32** 1442 (1957) [Reprinted in *Solitons and Particles*, Eds. C. Rebbi and G. Soliani (World Scientific, Singapore, 1984), p. 356]; H. Nielsen and P. Olesen, Nucl. Phys. **B61** 45 (1973) [Reprinted in *Solitons and Particles*, Eds. C. Rebbi and G. Soliani (World Scientific, Singapore, 1984), p. 365].
- [5] M. Shifman and A. Yung, Rev. Mod. Phys. **79**, 1139 (2007), [arXiv:hep-th/0703267]; an expanded version in *Supersymmetric Solitons*, (Cambridge University Press, 2009).

- [6] M. Shifman and A. Yung, *Lessons from Supersymmetry: Instead-of-Confinement Mechanism*, Int. J. Mod. Phys. **A29**, 1430064 (2014) arxiv:1410:2900 [hep-th].
- [7] A. A. Penin, V. A. Rubakov, P. G. Tinyakov and S. V. Troitsky, *What becomes of vortices in theories with flat directions*, Phys. Lett. B **389**, 13 (1996) [hep-ph/9609257].
- [8] A. Yung, *Vortices on the Higgs Branch of the Seiberg-Witten Theory*, Nucl. Phys. B **562**, 191 (1999) [hep-th/9906243].
- [9] K. Evlampiev and A. Yung, *Flux Tubes on Higgs Branches in SUSY Gauge Theories*, Nucl. Phys. B **662**, 120 (2003) [hep-th/0303047].
- [10] A. I. Vainshtein and A. Yung, *Type I superconductivity upon monopole condensation in Seiberg-Witten theory*, Nucl. Phys. B **614** (2001) 3 [hep-th/0012250].

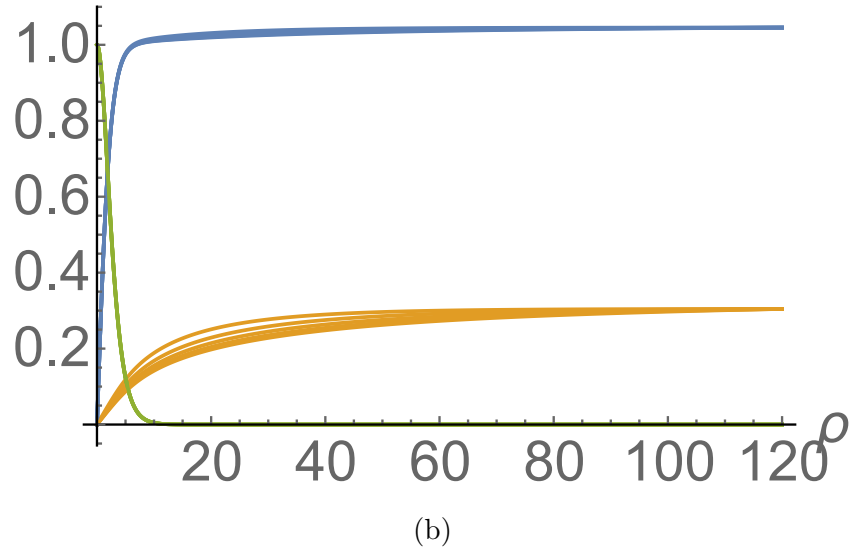
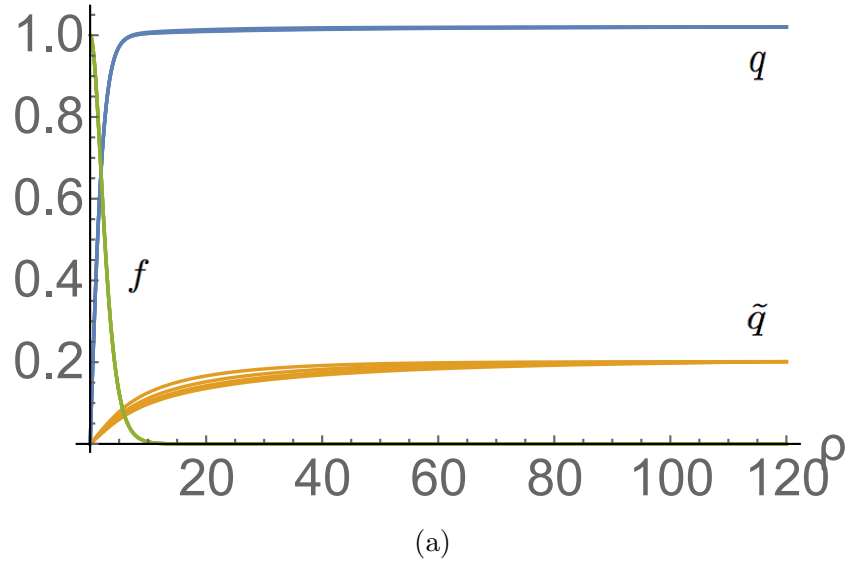


Figure 2: Numerical solutions for field profile functions varying m_L , the curve labels in (a) also apply to plot (b). In (a) we use $\rho_0 = 0.2$ and in (b) we pick $\rho_0 = 0.3$. The values of m_L used are reported in Figure 1.

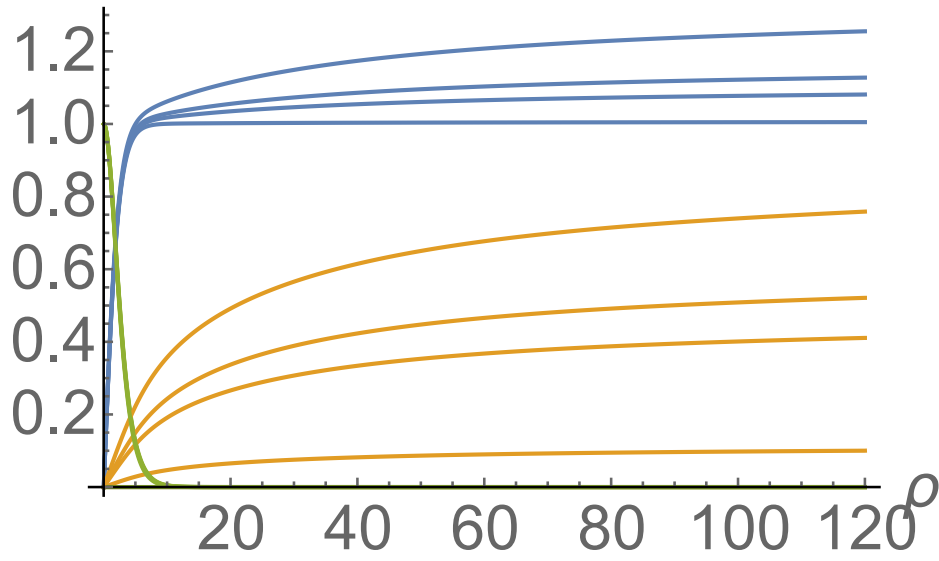


Figure 3: Field profiles varying ρ_0 at $m_L = 0.017$. The plots correspond to $\rho_0 = 0.1, 0.3, 0.4, 0.7$.

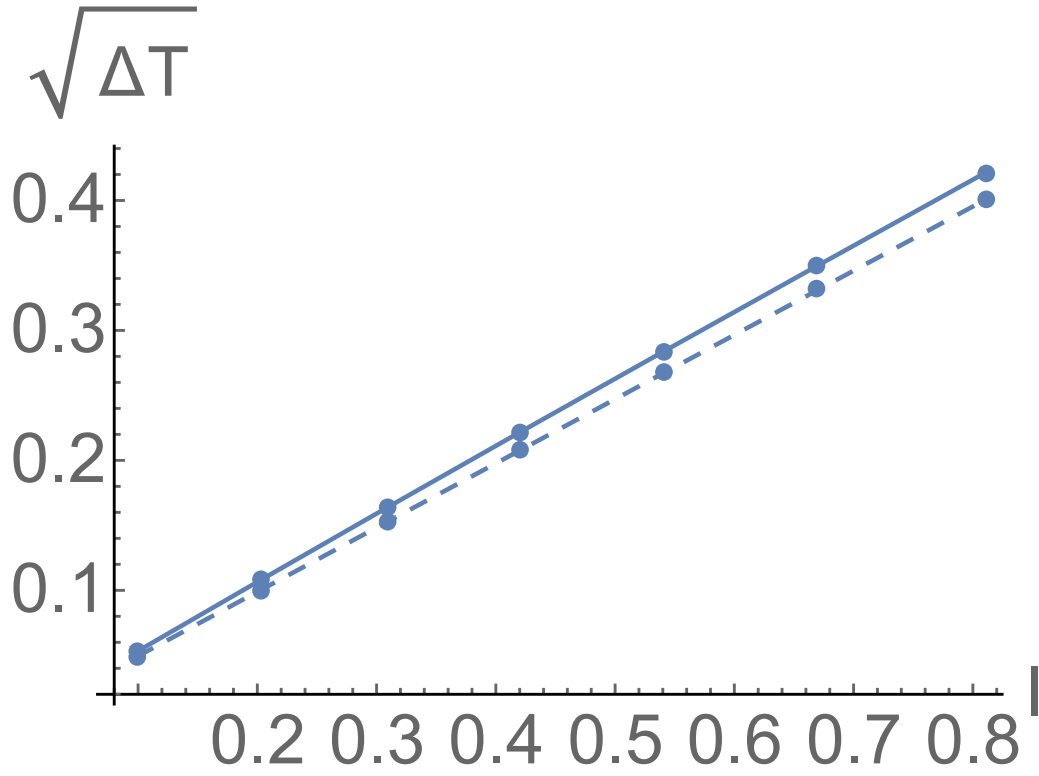
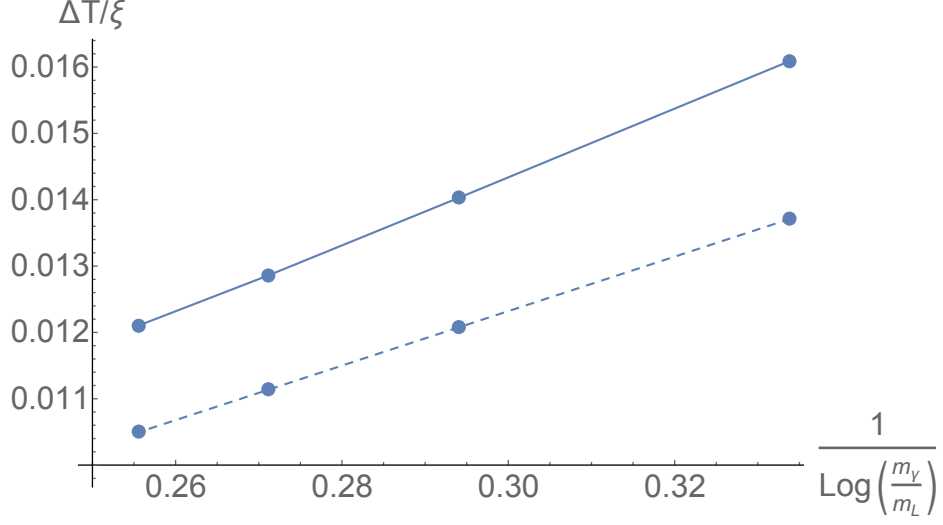
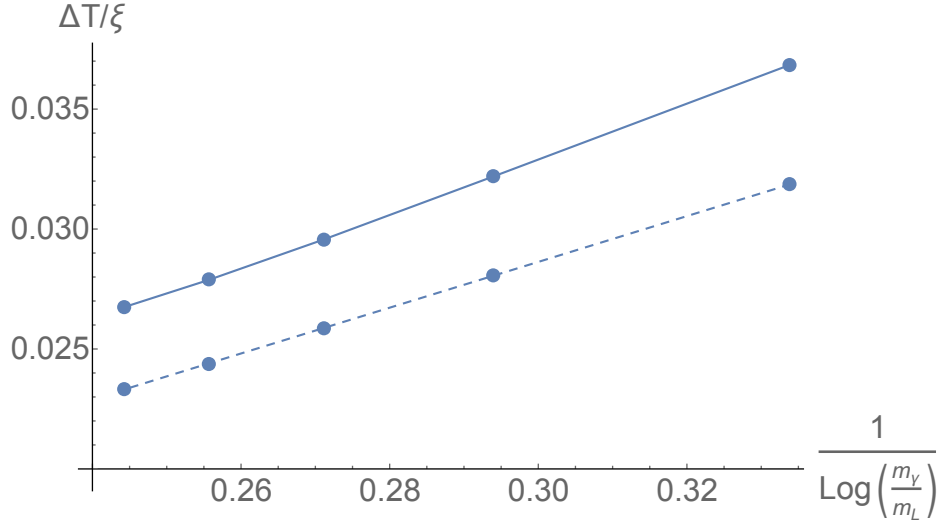


Figure 4: Difference between numerical and theoretical tensions $\Delta T/\xi$ for varying l . Solid line corresponds to numerical result, dashed line to theoretical. The values of ρ_0 used are 0.1 to 0.7 in steps of 0.1.



(a)



(b)

Figure 5: Difference between numerical and theoretical tensions ΔT for varying m_L . Solid line corresponds to numerical result, dashed line to theoretical. (a) $\rho_0 = 0.2$. (b) $\rho_0 = 0.3$. The values of m_L used are reported in Figure 1, plot (a) excludes the point in which our numerical procedure could not determine a solution.